Changes in Vegetation Condition and Surface Fluxes during NAME 2004

CHRISTOPHER J. WATTS,* RUSSELL L. SCOTT,+ JAIME GARATUZA-PAYAN,# JULIO C. RODRIGUEZ,@ JOHN H. PRUEGER,& WILLIAM P. KUSTAS,** AND MICHAEL DOUGLAS++

* *University of Sonora, Hermosillo, Mexico*
+ *USDA/Agricultural Research Service, Tucson, Arizona*
# *Instituto Tecnológico de Sonora, Ciudad Obregón, Mexico*
@ *Instituto del Medio Ambiente del Estado de Sonora, Hermosillo, Mexico*
& *USDA/Agricultural Research Service, Ames, Iowa*
** *USDA/Agricultural Research Service, Beltsville, Maryland*
++ *NOAA/National Severe Storms Laboratory, Norman, Oklahoma*

(Manuscript received 15 December 2005, in final form 21 June 2006)

ABSTRACT

The vegetation in the core region of the North American monsoon (NAM) system changes dramatically after the onset of the summer rains so that large changes may be expected in the surface fluxes of radiation, heat, and moisture. Most of this region lies in the rugged terrain of western Mexico and very few measurements of these fluxes have been made in the past. Surface energy balance measurements were made at seven sites in Sonora, Mexico, and Arizona during the intensive observation period (IOP) of the North American Monsoon Experiment (NAME) in summer 2004 to better understand how land surface vegetation change alters energy flux partitioning. Satellite data were used to obtain time series for vegetation indices and land surface temperature for these sites. The results were analyzed to contrast conditions before the onset of the monsoon with those afterward. As expected, precipitation during the 2004 monsoon was highly variable from site to site, but it fell in greater quantities at the more southern sites. Likewise, large changes in the vegetation index were observed, especially for the subtropical sites in Sonora. However, the changes in the broadband albedo were very small, which was rather surprising. The surface net radiation was consistent with the previous observations, being largest for surfaces that are transpiring and cool, and smallest for surfaces that are dry and hot. The largest evaporation rates were observed for the subtropical forest and riparian vegetation sites. The evaporative fraction for the forest site was highly correlated with its vegetation index, except during the dry spell in August. This period was clearly detected in the land surface temperature data, which rose steadily in this period to a maximum at its end.

1. Introduction

The North American monsoon (NAM) is an important regional phenomenon that provides the majority of annual rainfall over large parts of western Mexico and the southwestern United States. The premonsoon conditions in this region are of extreme dryness, with very high air temperatures and little or no rainfall occurring in the months before the arrival of the monsoon rains. The onset of the monsoon typically occurs in early June in the coastal areas of the Mexican states of Jalisco and Colima (around 20°N) before gradually moving northward, reaching southern Arizona in early July (around 35°N) (Douglas et al. 1993). Thus, the core monsoon region (Higgins et al. 2006), where the largest effects of the monsoon have been observed, has been roughly identified as the region between latitudes 20°–35°N and longitudes 100°–115°W with its center in the Sierra Madre Occidental (SMO), although there are also significant effects in other areas [e.g., monsoon onset is associated with a reduction in rainfall for the central region of the United States; Higgins et al. (1997)]. There is a scarcity of hydrometeorological data in the core region and it is essential to have better information about the basic variables: precipitation and evaporation. In the last few years, an event-based rain gauge network has been installed in order to augment the network of climate stations operated by the Mexican National Water Commission and the U.S. National Weather Service,

Corresponding author address: Christopher J. Watts, Departamento de Física, Universidad de Sonora, Blvd. Encinas y Rosales, Hermosillo, Sonora 83000, México.
E-mail: watts@fisica.uson.mx

DOI: 10.1175/JCLI4088.1

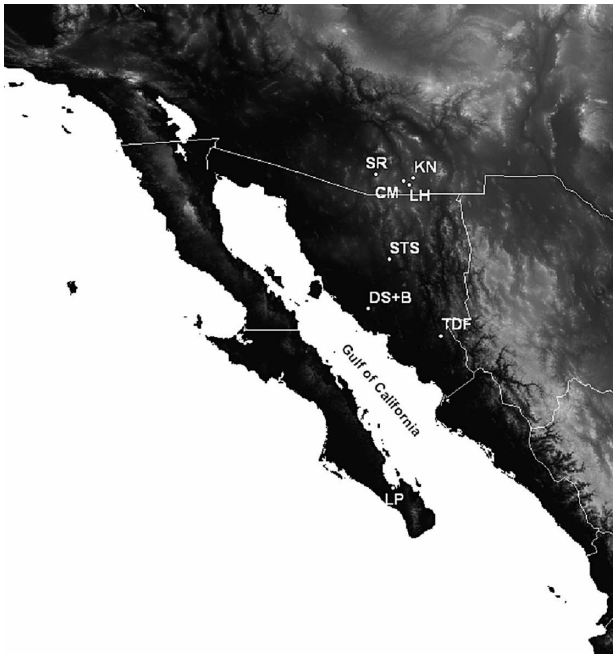

FIG. 1. Map of measurement sites for surface fluxes. Each site is displayed using the label from Table 1 and the background is a grayscale rendering of a Digital Elevation Model.

providing new insights into the space–time characteristics of the rainfall in this area (Gochis et al. 2004). Measurements of evaporation are much more difficult and very few have been made in the region, mainly in agricultural areas to study the consumptive use of important crops such as wheat, cotton, and grapes. Nonetheless, two previous campaigns over natural vegetation in the region should be mentioned: a study over desert shrub at the La Posa site near Hermosillo in 1995 (Stewart et al. 1998) and the Semi-Arid Land-Surface-Atmosphere (SALSA) campaign over grassland and shrubland in the San Pedro catchment in 1997–98 (Chehbouni et al. 2000). Neither of these campaigns was specifically designed to study the monsoon system.

The intensive observation period (IOP) for NAME took place in the period July–September 2004 and a small network of flux stations (Fig. 1) were set up in the core monsoon region in order to study the exchange of radiation, heat, and water vapor between the surface and the atmosphere in this area for several important biomes. One of the most significant is the tropical deciduous forest (TDF), which is found at midelevations on the western slopes of the Sierra Madre Occidental (SMO) as far north as 30°N. The TDF shows particularly dramatic changes with the onset of the monsoon, with extremely rapid leaf development. The TDF is generally located in regions of high rainfall intensity and there has been considerable speculation about possible land–atmosphere feedback mechanisms (Douglas et al. 2006). A site (TDF) was selected near Tesopaco, Sonora, in order to study these mechanisms in more detail. Another site was selected as part of the Soil Moisture Experiment 2004 (SMEX04) in the Sonora River basin. The southern part of this watershed contains subtropical shrub, which also responds very rapidly to the monsoon rains, and a site (STS) was selected near Rayón, Sonora. The last site in Sonora was chosen in a desert shrub area some 60 km south of Hermosillo as part of an ecological study into Buffel grass encroachment. Four sites were also monitored in southern Arizona, including a long-term riparian mesquite woodland site (CM) along the San Pedro River (see Scott et al. 2004 for details) and an upland mesquite savannah site (SR) in the Santa Rita Experimental Range. The other two U.S. sites were located in the Walnut Gulch Experimental Watershed operated by the Agricultural Research Service of the U.S. Department of Agriculture: a warm-season grassland site at Kendall (KN) and a desert shrub site at Lucky Hills (LH).

The purpose of this paper is to present results from the seven micrometeorological sites that were operating in the core monsoon region during the NAME IOP during the summer of 2004, in order to show how the partitioning of available energy was affected by the monsoon at a number of representative biomes. In section 2, there is a description of the instrumentation used at the sites and the data processing methodology. Section 3 contains an overview of the vegetation changes in the region as observed by satellite sensors [the *SPOT-5* VEGETATION program and the *Terra* Moderate Resolution Imaging Spectroradiometer (MODIS)] using vegetation indices. Section 4 presents an overview of the precipitation while section 5 describes the behavior of the surface albedo and net radiation at the sites. The energy balance and evapotranspiration over each surface are described in section 6. The relation between evaporative fraction and the vegetation index is discussed in section 7 and behavior of the surface temperature as observed by the *Aqua* MODIS satellite sensor in section 8. Finally, section 9 provides a summary of the results over the entire NAME IOP.

2. Surface flux site description

The sites were selected to include important biomes in the region: desert shrub (LH, DS+B), grassland (KN), savannah (SR), subtropical shrub (STS), and tropical deciduous forest (TDF). Surface fluxes of sensible heat and water vapor were measured at all sites

TABLE 1. Summary of characteristics of flux sites in Arizona and Sonora.

Site	Vegetation type	Location	Lat (°N)	Lon (°W)	Net radiometer	Hygrometer
CM	Riparian woodland	Near Charleston, AZ	31.66	110.18	CNR1	LI7500
LH	Desert shrub	Lucky Hills Subwatershed, Walnut Gulch Experimental Watershed, Tombstone, AZ	31.74	110.05	CNR1	LI7500
KN	Grassland	Kendall Subwatershed, Walnut Gulch Experimental Watershed, Tombstone, AZ	31.74	109.94	CNR1	LI7500
SR	Savannah	Santa Rita Experimental Range, Green Valley, AZ	31.87	110.82	CNR1	
TDF	Tropical deciduous forest	Tesopaco, Sonora	27.85	109.30	CNR1	LI7500
STS	Subtropical shrub	Rayón, Sonora	29.74	110.54	CNR1	KH20
DS+B	Desert shrub with Buffel grass	La Pintada, Sonora	28.52	111.06	NRLite	KH20

using the eddy covariance (EC) method, which requires high-frequency samples of vertical wind speed (w), air temperature (T), and humidity (q). These data are used to calculate the covariance functions Cov(w, T) and Cov(w, q), which are proportional to the fluxes of heat and water vapor, respectively. These covariance values are more accurate when determined over long time periods (several hours) but the diurnal variations in the variables require shorter periods, usually chosen to be between 10 min and 1 h.

The other principal components of the surface energy balance, net radiation, and soil heat flux were also measured. The sensors for net radiation, air temperature, and water vapor were installed several meters above the canopy at each site and so the measured surface fluxes are representative of the exchange of radiation, heat, and water vapor between the soil–vegetation complex and the atmosphere. The choice of instrumentation was not uniform for all sites, with the most important differences for net radiation and water vapor concentration. The preferred net radiometer was the CNR1 (Kipp & Zonen, Delft, the Netherlands), which provides independent measurements of all four components: incoming and outgoing radiation in short- and longwave bands. At one site (DS+B), however, a simpler net radiometer (NRLite, Kipp & Zonen) was installed to measure only the total net radiation. The preferred instrument for measuring the water vapor concentration was the LI7500 gas analyzer (LI-COR, Lincoln, Nebraska), which provides simultaneous measurements of both water vapor and carbon dioxide. However, some sites used the KH20 Krypton hygrometer KH20 [Campbell Scientific Inc. (CSI), Logan, Utah).

All sites were equipped with a three-dimensional sonic anemometer CSAT3 (CSI) and the flux data were sampled at all sites at a frequency of 10 Hz using a CR5000 datalogger (CSI). The CR5000 is programmed to calculate 30-min averages for the fluxes, but it also includes a Compact Flash card so that the raw data can be stored and analyzed later. Many procedures have been suggested for processing eddy covariance data and their definition remains an important topic for research. The interested reader will find a thorough discussion of these issues in the recent *Handbook of Micrometeorology* (Lee et al. 2004). The specific procedures used for the data from these sites are described in a previous paper (Scott et al. 2004) and are confined to simple data-filtering, axis rotation so that the mean vertical wind speed is zero for each period and corrections for fluctuations in air density. (At sites with krypton hygrometers, the data were also corrected for oxygen absorption.) The present study does not include any data analysis for carbon dioxide. The information about the instrumentation at each site is shown in Table 1.

Each site included sensors buried in the soil to measure soil temperature, humidity, and heat flux. The soil at the TDF site is shallow and full of volcanic rocks, so that we were not able to install soil moisture sensors at depths below 3 cm. These characteristics of the soil may be a significant factor in the existence of the TDF farther north than one might expect, because sites with very rocky soils allow rapid infiltration of precipitation away from the soil evaporation zone, which is available later to sustain plant growth (see Holbrook et al. 1995). In effect the rainfall is concentrated into the spaces between the rocks where the roots are situated, so that more water is available to the roots than would be the case in a more homogeneous soil.

3. Vegetation changes

Dramatic increases in foliage for many plants can be observed with the onset of the summer rains. These

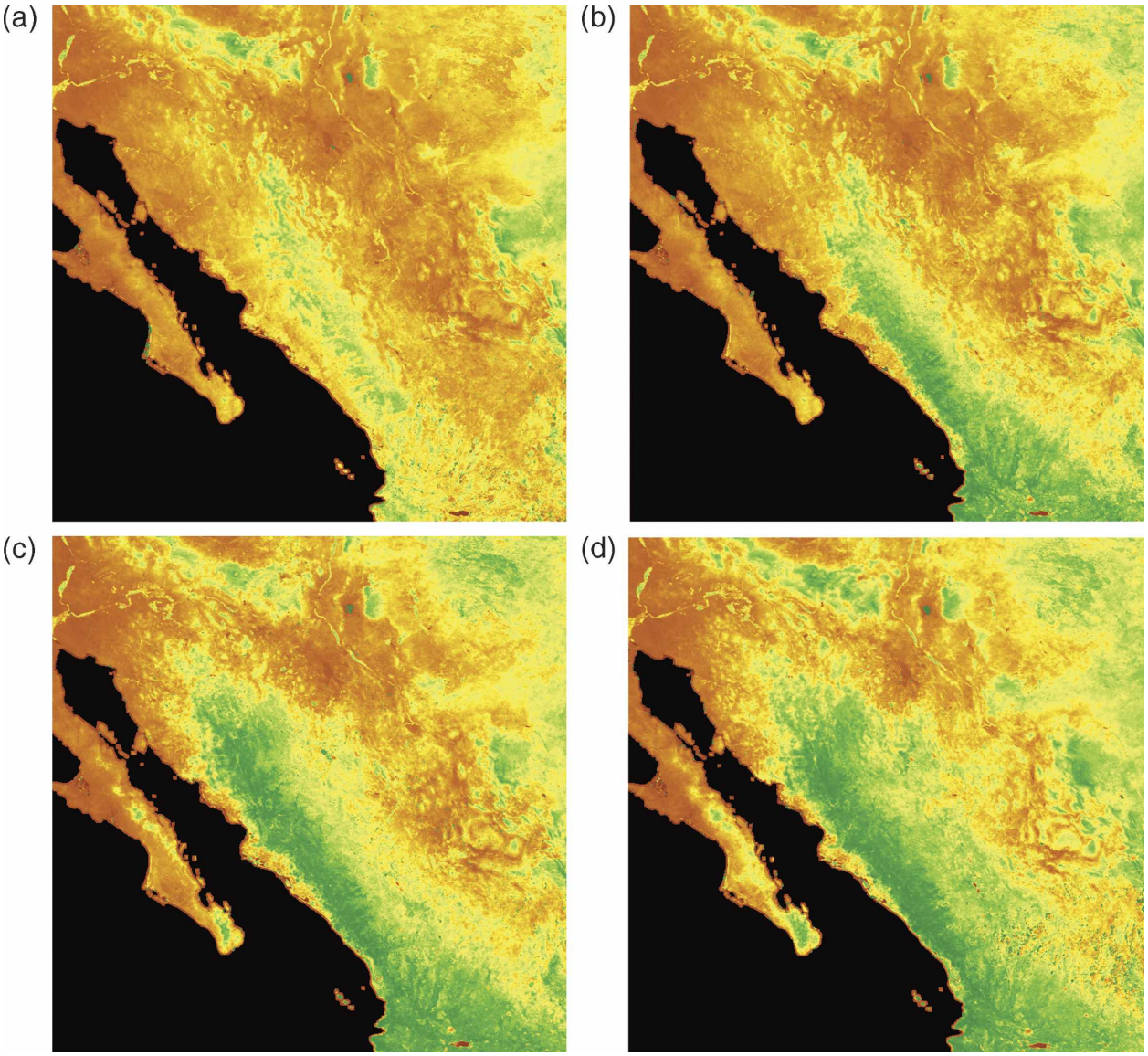

FIG. 2. Display of NDVI data for the land surface from the *SPOT-5* VEGETATION sensor for the core monsoon region (20°–35°N, 100°–115°W) in 2004. A color scale is used (ocean is black) with tones from brown to green. Each image is a composite of the first 10 days of the month: (a) June, (b) July, (c) August, and (d) September.

changes can be conveniently monitored and quantified using vegetation indices calculated from optical satellite data that exploit the differences in the reflectance of vegetation in the red (ρ_{red}) and near-infrared (ρ_{nir}) bands. Many vegetation indices have been defined but the most popular continues to be the normalized difference vegetation index (NDVI):

$$\mathrm{NDVI} = \frac{\rho_{nir} - \rho_{rojo}}{\rho_{nir} + \rho_{rojo}}. \quad (1)$$

We obtained data from the SPOT-VEGETATION sensor (the data can be downloaded without charge online at http://free.vgt.vito.be/). These data are 10-day composites with a spatial resolution of around 1 km. The global data are separated into 10 regional files and the Central America region (0°–50°N, 50°–125°W) was used. Software (developed at IUAV, Venice, Italy) is available at this site to extract a subregion from the compressed file. The evolution of NDVI over the core monsoon region (20°–35°N, 100°–115°W) is displayed in Fig. 2 for the first 10 days of each month from June through September. In early June, the green-up is patchy along parts of the Sierra Madre Occidental (SMO). By early July there is an extensive green area

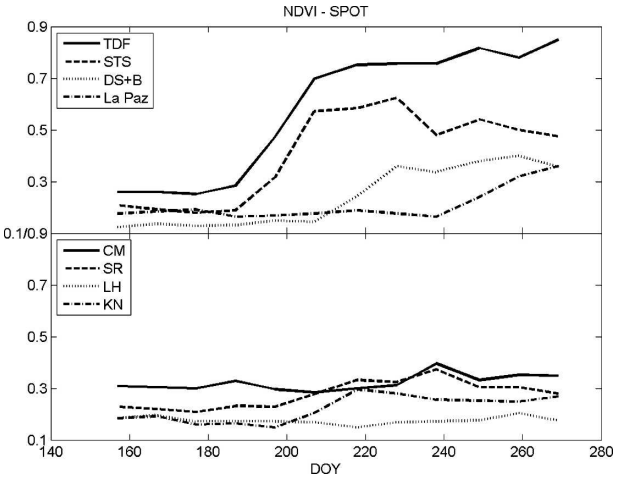

FIG. 3. The 10-day composite NDVI values for each of the sites derived from the *SPOT-5* VEGETATION satellite sensor.

along the coast and inland in the southern part as well as along the upper levels of the SMO. By early August, this green-up extends down the western slopes of the SMO as well as farther northward, and by early September, the green area becomes maximum with further extensions to the north and east. This general pattern is very similar to the observed rainfall in the area (Douglas et al. 1993; Gochis et al. 2004)

The NDVI images from *SPOT-5* were processed (using the IDRISI software packet developed at Clark University, Worcester, Massachusetts) to generate the time series for the three sites in Sonora and the four sites in Arizona that are displayed in Fig. 3 using the day of the year (DOY). (The relation between the calendar date and DOY is shown for convenience in Table 2.) The long-term Ameriflux site in desert shrub near La Paz (Hastings et al. 2005) is also shown for reference. The response to the monsoon conditions is seen in the period 10–20 July (DOY 192–202) for the TDF and STS sites but a month later at the DS+B site. In addition, the maximum values for NDVI at each site are 0.85 for TDF, 0.62 for subtropical shrub (STS), and 0.4 for desert shrub with Buffel grass (DS+B), where these values are indicative of the maximum ground cover attained at each site. The vegetation at the La Paz desert shrub site responds much later than the others, with an increase of 0.2 in September. The data for the Arizona sites show a much smaller response, with NDVI values between 0.15 and 0.4 at all three sites. An increase of 0.15 in NDVI is observed for the riparian woodland (CM) and grassland (KN), 0.12 for the savannah (SR), and only 0.05 for desert shrub (LH). We believe that these values are representative of the surface/vegetation conditions at all sites *except* for the riparian woodland site (CM), because this vegetation type is confined to a narrow strip around the river and higher spatial resolution is required.

TABLE 2. Relation between calendar date and DOY.

Calendar date	DOY
1 Jul	183
15 Jul	197
1 Aug	214
15 Aug	228
1 Sep	245
15 Sep	259
1 Oct	275

The enhanced vegetation index (EVI; Huete et al. 2002) corrects for some distortions in the reflected light caused by the particles in the air as well as the ground cover below the vegetation. Also the EVI data do not become saturated as easily as the NDVI data when viewing rain forests and other areas of the earth with large amounts of chlorophyll. The EVI was developed for use with the MODIS sensor, which is on board both the *Terra* and *Aqua* satellites. The *Aqua* satellite has a nominal local overpass time during the day of 1330 LT while the *Terra* overpass is around 1030 LT. We decided to use the 16-day composite product with a spatial resolution of 250 m from the *Terra* satellite (MOD13Q1). All MODIS products are freely available online at the National Aeronautics and Space Administration Distributed Active Archive Center (NASA DAAC) Web sites. Figure 4 shows EVI values for our sites and we see that, although they are generally lower than the corresponding NDVI (since EVI was designed to avoid some of the latter's saturation problems), the general behavior for each of the indices is very similar. As expected, the values of EVI for the riparian woodland site are significantly higher relative to EVI at the other sites, while its seasonal variation is modest. Therefore, these EVI values at a higher spatial resolution are probably more reliable and representative than the lower spatial resolution NDVI values in Fig. 3.

4. Precipitation

Weekly precipitation at all the sites is shown in Fig. 5 and it should be remembered that the data for the Sonora sites were only available after DOY 192–196. Clearly the rainfall at the TDF site is much larger than at any of the others. The maximum monsoonal rainfall occurs in late July for the TDF and Arizona sites, but not until 2–3 weeks later at the STS and DS+B sites. An interesting feature is the 3-week period with virtually no rainfall at the TDF site during August. Shorter 2-week gaps are also observed slightly later at the STS

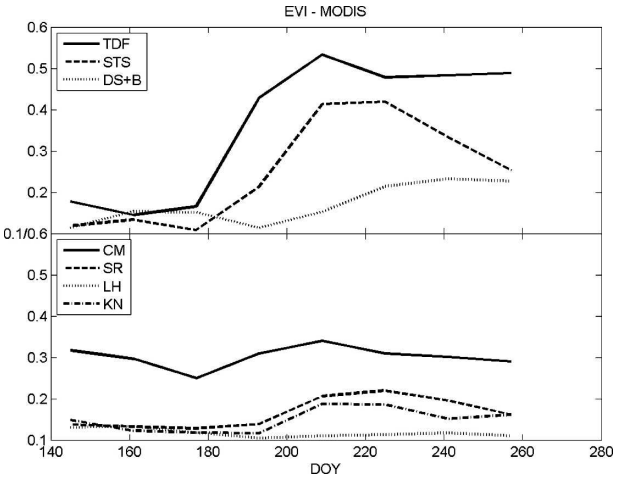

FIG. 4. The 16-day composite EVI values at the sites derived from 250-m bands of the MODIS sensor on the *Terra* satellite.

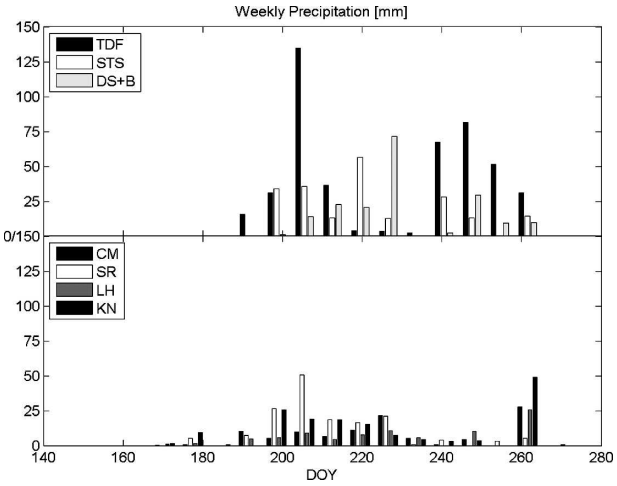

FIG. 5. Precipitation at all the sites in the period June–September 2004. Note that there are no data at the Sonora sites before 10 July (DOY 192).

and DS+B sites. The so-called midsummer drought is a regular occurrence in southern Mexico (Magaña et al. 1999) but it is not usual in northwest Mexico. Indeed the end of this condition coincided with the arrival of Hurricanes Howard (DOY 234–240) and then Javier (DOY 245–252), and it is difficult to separate the effects of these from those of the monsoonal circulations. The southern Arizona sites show much lower rainfall with the largest values at the savannah site. The rainfall was concentrated in a 6-week period between mid-July and late August and suggests that the rainfall in late September is due to the indirect effects of tropical storms.

The observed distribution of the rainfall is consistent with the changes in vegetation discussed previously. It is notable that the tropical vegetation responds much more rapidly and vigorously to the rainfall than any other type, with the behavior of the SR, KN, and DS+B sites being quite similar. The riparian CM site also responds early but the rainfall plays a less important role on the greenness of this site since the woodland overstory has access to a stable source of groundwater throughout the year. The lowest rainfall was recorded at the LH site and this also showed the smallest changes in seasonal vegetation conditions before and after the onset of the monsoon.

5. Available energy at the surface

The net radiation at the surface may be separated into its short- and longwave components and written as

$$R_n = (1 - \text{albedo})R_s - R_{\text{nl}}, \quad (2)$$

where the albedo is the shortwave reflectance integrated over all wavelengths, R_s is the incoming solar radiation, and R_{nl} is the net longwave radiation, defined here as outgoing minus incoming longwave radiation, which means that it is usually positive. Since the incoming solar radiation at all the sites is quite similar, the main factors that influence the available net radiation are 1) the albedo of the surface; 2) the surface temperature, which determines the upward component of the net longwave radiation, R_{nl}; and 3) the near-surface air humidity, which affects the downward component of the net longwave radiation. All components of net radiation were continuously measured at six of the sites and we can study these in detail.

Broadband albedo was measured at all the sites except the DS+B site and Table 3 contains values for these sites before and after the monsoon rains. Under dry conditions, the differences in albedo between the different biomes show about a twofold difference, from the lowest in TDF to the highest in desert grassland (KN) and shrub (LH). After the monsoon onset, the Sonoran sites show a small increase in albedo (2%–3%) while the Arizona sites show a small decrease (1%).

TABLE 3. Comparison of measured albedo (%) values at the sites.

Site	Premonsoon onset	Postmonsoon onset
Tesopaco TDF	9	12
Rayon STS	15	17
CM riparian woodland	10	8
SR savannah	15	14
KN grassland	18	17
LH desert shrub	18	17

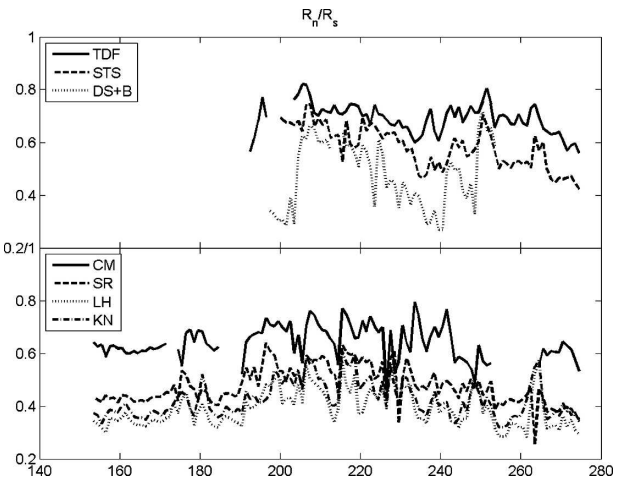

FIG. 6. The behavior of net radiation (expressed as a fraction of incoming solar radiation) for all the sites.

Thus, the albedo values for these biomes only exhibit very small *seasonal* changes, even though the monsoon rains produce significant physiological changes and increases in leaf area. Moreover, at the subtropical vegetation sites in Sonora (TDF and STS) where the largest changes occur, the albedo values increase when one might have expected a decrease due to the greener/darker canopy and the wetter soil. However, the soils in these biomes have a large organic content and are generally quite dark in color so that the main change is the increase in the leaf area. Presumably, the increase in light reflected by the leaves in the near-infrared region more than offsets their increased absorption in the visible bands. Finally, we should note that albedo changes may well be larger for the DS+B site, since the soil there is light colored and the growth of the Buffel grass produces a significant change in ground cover.

If the net radiation is expressed as a fraction of the incoming solar radiation, we have

$$\frac{R_n}{R_s} = 1 - \text{albedo} - \frac{R_{\text{nl}}}{R_s}, \tag{3}$$

so that much of the high-frequency variability due to cloudiness is removed from the data. Thus, the net radiation will be a larger fraction of the incoming solar radiation if the albedo and net longwave radiation are small. In general, this will be the case for surfaces that are wet and cool. Figure 6 shows the behavior of this fraction for all the sites. The highest values are obtained for the TDF (0.57–0.83) and the riparian woodland CM (0.58–0.80), as compared to the STS (0.42–0.75), DS+B (0.28–0.71), SR (0.32–0.63), and finally KN (0.37–0.60) and LH (0.28–0.59). In general, there is an increase in this fraction after the rains but this is relatively modest for the sites in Arizona. The most dramatic increase is observed at the DS+B site: 0.33 in just 2 days after the first rains. This site is also the only one where there is a clear signal for the dry period after DOY 220 when this fraction decreases from around 0.6 to 0.2 in 20 days. As noted previously, changes in albedo may be important at this site. At all of the other sites we have seen that the albedos are relatively constant over time, so that the variation in the available energy as a fraction of incoming solar radiation must be due mainly to the net longwave component. In other words, the driest and hottest sites are the desert shrub (LH) and grassland (KN), where as little as 30% of the incoming solar radiation is available at the surface, while the wettest and coolest sites are the tropical forest (TDF) and riparian woodland (CM), where as much as 80% of the incoming solar radiation is available at the surface. The reduction observed at the end of September is mainly due to a seasonal reduction in atmospheric water content, which in turn reduces the downward longwave radiation to the surface.

6. Evapotranspiration (ET)

In the absence of horizontal advection and assuming there is no change in energy storage, the energy balance at the surface is usually written,

$$R_n = G + H + \text{ET}, \tag{4}$$

where the net radiation at the surface (R_n) may be used for heating the soil (G), for heating the atmosphere (H), and for evapotranspiration (ET). When daily average fluxes are considered, the soil heat flux G is generally very small and may be neglected. All these terms are energy fluxes expressed in watts per meter squared although other units may be used and it is often convenient to express them as equivalent evaporation in millimeters.

The ET data for all the sites are displayed in Fig. 7. The riparian woodland site (CM) is different from the others since the vegetation here has a continuous supply of water throughout the year, so that there is very little seasonal change during the summer months and ET varies between 1.7 and 5.2 mm day^{-1} according to the atmospheric demand. This behavior is in stark contrast to the other sites in southern Arizona where ET is very small ($<$0.5 mm day^{-1}) at all the sites at the beginning of June. Each rainfall event produces a rapid response from the vegetation (data not shown) with ET reaching maximum values of 4.4 mm day^{-1} at the savannah site (SR), 3.3 mm day^{-1} at the grassland site (KN), and 2.4 mm day^{-1} at the desert shrub site (LH). The behavior of ET for the northern sites is in contrast

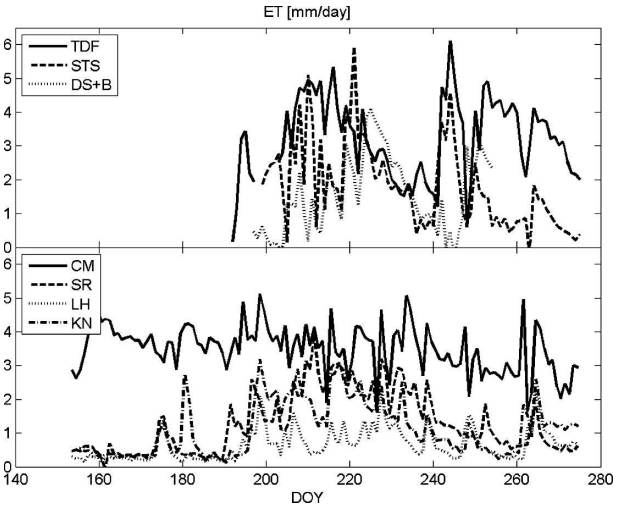

FIG. 7. Evapotranspiration (mm) for all the sites for the period June–September 2004.

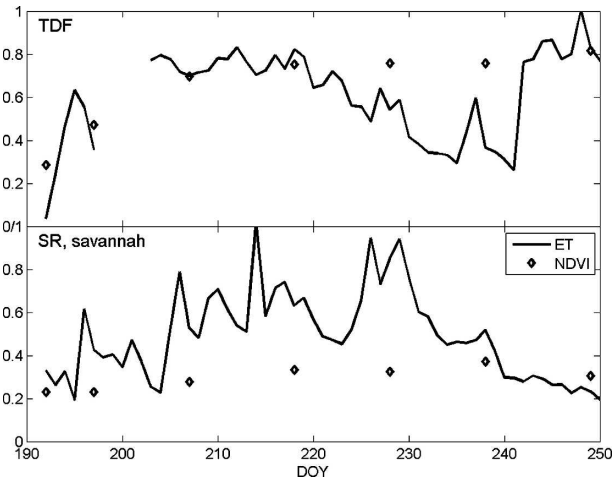

FIG. 8. Evaporative fraction (EF) and NDVI at the TDF near Tesopaco, Sonora, for the period July–September 2004.

to the more tropical, southern sites. Unfortunately, we were not able to install the instrumentation at the Sonora sites until mid-July and ET, although small initially at all three sites, started to rise immediately at both the STS and TDF sites, so that the only site to have a good record for the dry season is DS+B. Nonetheless, not much rain had fallen before the installation so that the main features are still apparent in Fig. 7. One striking feature common to all Sonoran sites is the sharp decrease in ET during August. This coincides with the sharp reduction in rainfall at these sites as observed in section 4. We can observe quite different behavior at each site. The maximum daily ET is around 6 mm at both the TDF and STS sites, while it is 4 mm for the DS+B site. The response to rainfall *pulses* is apparent at the STS and DS+B sites with much faster dry-out at the latter. It is apparent that the TDF is able to maintain high rates of ET for longer periods after a rain event, indicating that the root systems are able to access soil moisture for several days to weeks before any water stress occurs. This contrasting behavior at the sites can be most clearly seen for the period DOY 260–280. Here, a regional rainfall event produced responses at all the sites with much faster dry-out in the upland desert sites (SR, KN, LH) than the tropical sites (STS, TDF).

7. Evaporative fraction and NDVI

The partition of the available energy between sensible heat H and latent heat ET is an important surface property that may be described using the Bowen ratio (B), defined as

$$B = \frac{H}{\mathrm{ET}}, \tag{5}$$

or the evaporative fraction (EF), defined as

$$\mathrm{EF} = \frac{\mathrm{ET}}{\mathrm{ET} + H} = \frac{1}{1 + B}. \tag{6}$$

Since each parameter contains precisely the same information, either one may be used. On a daily basis, the net heating of the soil is usually much smaller than the other components and may be neglected. In this case we may use the energy balance to write

$$\mathrm{EF} = \frac{\mathrm{ET}}{R_n - G} \approx \frac{\mathrm{ET}}{R_n}. \tag{7}$$

If there is closure in the energy balance, the two expressions for EF [Eqs. (6) and (7)] are exactly equal. In practice, it is common that the energy balance does not close (Twine et al. 2000) so that each expression gives slightly different results. We can see that the EF is *normalized* ET with respect to differences in net radiation. It is also much less noisy than ET since clouds will tend to reduce all these terms more or less in the same proportion. Moreover, in the absence of advection, the net radiation represents an upper limit for ET since we can assume in this case that the minimum sensible heat flux H will be close to zero. Thus, EF is normally constrained to lie between 0 and 1, where EF = 0 for completely dry conditions and EF = 1 for wet conditions with maximum ET. Figure 8 shows the results from the TDF and SR sites together with the NDVI from satellite data for each site. At the TDF site we can see that the general behavior is represented quite well by NDVI while the foliage is increasing. However, NDVI values remain constant throughout the periods

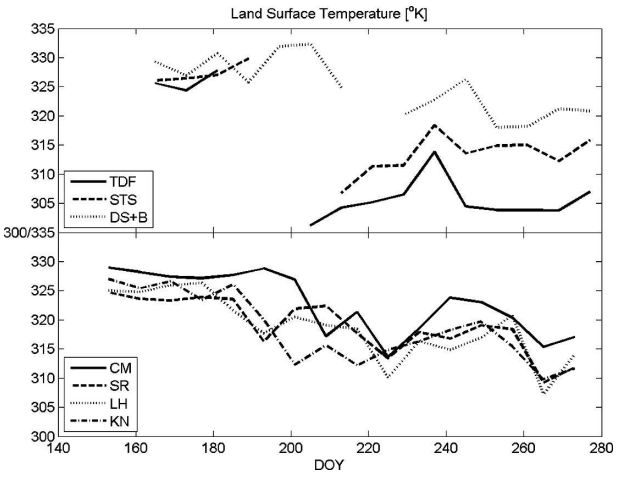

FIG. 9. Land surface temperature (K) derived from the MODIS sensor on the *Aqua* satellite. The spatial resolution is 1 km and the local overpass time is around 1330 LT.

of water scarcity in August and then in late September. It is clear that a much more prolonged dry period would be required in order for this to be observable in the NDVI values. In other words, only when the leaves turn yellow and wilt would we observe any important change in vegetation index. It would seem that the only possible source of useful satellite data would be the surface temperature, since this would be expected to react much more quickly to water scarcity with an increase in leaf temperature. The SR site shows the response to rainfall pulses mentioned above that is typical of all of the other sites. There would appear to be no useful relationship between the vegetation index and EF in this case.

8. Surface temperature

The MODIS sensor, which possesses many thermal channels that may be used to estimate the land surface temperature (LST), is on board both the *Terra* and *Aqua* satellites. Our goal is to observe plant water stress and this is generally proportional to the solar elevation, so that the 1330 LT overpass time for *Aqua* is better suited for this purpose. Figure 9 shows the daytime LST for the Sonora and Arizona sites, obtained from the 8-day composite product (MYD11A2), which has a spatial resolution of 1 km, from June through September 2004. In premonsoon conditions, LSTs at all the sites are between 320 and 330 K. After the onset of the monsoon, all of the temperatures are lower, with the largest differences in TDF (27 K) and STS (23 K); then SR (15 K), KN (14 K), and DS+B (12 K); and finally CM and LH (8 K). The Arizona sites show a strong, quasi-linear downward trend throughout this period, as the solar radiation forcing decreases in the fall.

An important feature is the data gap at the tropical sites corresponding to the periods DOY 182–197 for the TDF and DOY 190–205 at the STS site. This gap indicates that no cloud-free views of these sites were available during these periods, so that they can be associated with intense monsoon activity when LST was relatively low due to reduced solar heating. Note that the instruments at the TDF and STS sites were installed on DOY 192 and 197, respectively, and so we do not have field data at these sites for the most extreme dry conditions.

The temperature response can be related to the observed ET and rainfall pattern. Thus, LST increases during August to a maximum value of 314 K in the TDF and to 318 K in the STS during the 8-day period before DOY 240. Figure 7 shows that this corresponds to the lowest ET values at these sites before renewed rainfall at the end of August. For the DS+B site the maximum value of 326 K occurs in the following period after DOY 240 and Fig. 7 again shows that this corresponds to the minimum ET for that site. Therefore, the series of MODIS LST 8-day composite images shows a clear response to the extended dry period in August and provides useful information for monitoring ET. However, the rapid dry-out observed at the desert sites (DS+B, SR, KN, LH) means that more frequent (~daily) LST data would be required in order to monitor ET at these sites.

9. Summary of results

In this paper we have examined the relation between land surface and atmospheric properties using data from satellites and micrometeorological stations during the North American Monsoon Experiment in the summer of 2004. The values for several significant variables are summarized in Table 4 in both premonsoon and monsoon conditions. The monsoon onset occurs at slightly different times at these sites and is a function of latitude and elevation. Thus, the numbers in the table do not correspond to exactly the same dates at each site. Furthermore, it should be remembered that the measurements at the TDF and the STS started in mid-July, so that the premonsoon values are based on more limited data than for the other sites. The most significant results are listed below.

Satellite data give useful information about the relative monsoon intensity at different sites via the use of the observed increase in vegetation index (NDVI, EVI) and the decrease in surface temperature (LST). As expected, the largest values were obtained for the tropical vegetation, where $\Delta\text{EVI} = 0.4$ and $\Delta\text{LST} = -20$ K for the TDF and

TABLE 4. Summary of data for premonsoon and monsoon conditions.

	Sites						
	TDF	STS	DS+B	CM	SR	KN	LH
Premonsoon							
EVI (min)	0.14	0.11	0.12	0.26	0.12	0.11	0.10
LST (K)	325.9	327.5	328.8	323.8	327.9	325.7	324.7
R_n (W m^{-2})	177	169	80	171	142	118	107
ET (W m^{-2})	57	66	10	103	24	12	10
EF	0.38	0.30	0.10	0.69	0.20	0.11	0.10
Bowen ratio	2.6	2.3	9.0	0.4	4.0	8.1	9.0
Monsoon							
EVI (max)	0.54	0.42	0.23	0.34	0.22	0.20	0.12
LST (K)	305.4	313.3	321.1	316.3	318.9	314.8	315.3
R_n (W m^{-2})	190	176	132	148	134	113	105
ET (W m^{-2})	115	83	59	100	67	47	26
EF	0.75	0.56	0.54	0.75	0.56	0.50	0.27
Bowen ratio	0.3	0.8	0.9	0.3	0.8	1.0	3.7
Entire period							
P	434	207	172	103	159	157	87
ET/P	0.59	0.67	0.76	3.08	0.96	0.83	0.83

ΔEVI = 0.3 and ΔLST = -14 K for the STS. The smallest differences were observed at the riparian woodland (CM) site where ΔEVI < 0.1 and ΔLST = -7 K.

The rainfall follows a similar pattern, and the rainfall at the TDF site is more than twice as large as that at the STS site. The grassland and savannah sites (DS+B, KN, SR) have the next highest values, and the lowest rainfall rates are observed at the riparian and shrub sites (CM, LH). The rainfall in the TDF is 5 times that in LH! This is expected since the vegetation present at each site is in large part dependant on the amount of rainfall available there.

Continuous measurements of broadband albedo were obtained at all the sites except DS+B and the observed seasonal changes in the albedo were very small. The largest change (in the TDF) would increase net radiation by no more than 3% of the solar radiation, which is equivalent to about 0.3 mm of evaporation. So for most practical purposes, the albedo can be considered constant at these sites. This is surprising given the substantial changes observed for spectral reflectance of the vegetation (Figs. 2–4) and suggests to us that seasonal changes in albedo for natural vegetation in the region are not very important in terms of regional land–atmosphere interactions.

The net radiation only exhibits large changes at the DS+B sites. However, the satellite data show that the largest changes in LST occur at the tropical sites (TDF and STS) so that we would also expect to see significant changes there. Unfortunately, installation of the instruments at these sites was too late to obtain a good record of the extreme hot and dry conditions preceding the monsoon onset.

The highest evaporative fractions (0.75) in the monsoon period are observed in the riparian woodland and the TDF sites. However, the importance of the TDF in the regional hydrometeorology is much greater due to its spatial cover. The lowest response (0.27) was observed at LH and all the other sites had similar EF values in the range 0.50–0.56.

The ratio between evapotranspiration and precipitation (ET/P) may be used as a measure of the "efficiency" of an ecosystem's use of rainfall. The data for the riparian woodland (CM) stands out with 3 times as much ET as rainfall, indicating that the growth of this vegetation is independent of local precipitation. The subtropical vegetation is the least efficient (0.59–0.67), while the desert vegetation is the most efficient (0.76–0.96). These observations are consistent with the notion that for vegetation to survive in arid conditions, it must make optimum use the scarce rainfall available.

The results of this study contribute to a better understanding about the role of surface cover on monsoon dynamics and land–atmosphere feedbacks. The data will be important for evaluating and improving the performance of hydrometeorological models in the region. This knowledge will enable us to give answers to very practical questions about the impact of land cover changes on weather systems. For instance, what would

be the consequences if the TDF and desert shrub are replaced by Buffel grass?

Acknowledgments. The authors wish to acknowledge the assistance of Miguel Agustin Rivera, William Cable, and Ahmed Balogun in the installation of the instruments and data processing. The suggestions of the anonymous reviewers greatly improved the paper. Support for this work was provided by a NOAA/Office of Global Programs contract. Further support was provided by the U.S. Department of Agriculture's Agricultural Research Service and the PROMEP program of the Mexican Ministry of Education.

REFERENCES

Chehbouni, A., and Coauthors, 2000: A preliminary synthesis of major scientific results during the SALSA program. *Agric. For. Meteor.,* **105,** 311–323.

Douglas, M. W., R. A. Maddox, and K. Howard, 1993: The Mexican monsoon. *J. Climate,* **6,** 1665–1677.

——, J. F. Mejia, J. M. Galvez, R. Orozco, and J. Murillo, 2006: The seasonal evolution of the diurnal variation of the low-level winds around the Gulf of California. Is there a link to vegetation green-up during the wet season? Preprints, *18th Conf. on Climate Variability and Change,* Atlanta, GA, Amer. Meteor. Soc, CD-ROM, J3.4.

Gochis, D. J., A. Jimenez, C. J. Watts, J. Garatuza-Payán, and W. J. Shuttleworth, 2004: Analysis of 2002 and 2003 warm-season precipitation from the North American Monsoon Experiment rain gauge network. *Mon. Wea. Rev.,* **132,** 2938–2953.

Hastings, S. J., W. C. Oechel, and A. Mulia-Melo, 2005: Diurnal, seasonal and annual variation in the net ecosystem CO_2 exchange of a desert shrub community (Sarcocaulescent) in Baja California, Mexico. *Global Change Biol.,* **11,** 927–929.

Higgins, R. W., Y. Yao, and X. Wang, 1997: Influence of the North American monsoon system on the U.S. summer precipitation regime. *J. Climate,* **10,** 2600–2622.

——, and Coauthors, 2006: The North American Monsoon Experiment (NAME) 2004 field campaign and modeling strategy. *Bull. Amer. Meteor. Soc.,* **87,** 79–94.

Holbrook, N. M., J. L. Whitbeck, and H. A. Mooney, 1995: Drought responses of neotropical deciduous forest trees. *Tropical Deciduous Forests,* S. H. Bullock, H. A. Mooney, and E. Medina, Eds., Cambridge University Press, 468 pp.

Huete, A., K. Didan, T. Miura, E. P. Rodriguez, X. Gao, and L. G. Ferreira, 2002: Overview of the radiometric and biophysical performance of the MODIS vegetation indices. *Remote Sens. Environ.,* **83,** 195–213.

Lee, X., W. Massman, and B. Law, Eds., 2004: *Handbook of Micrometeorology: A Guide to Surface Flux Measurement and Analysis.* Kluwer Academic, 268 pp.

Magaña, V., J. A. Amador, and S. Medina, 1999: The midsummer drought over Mexico and Central America. *J. Climate,* **12,** 1577–1588.

Scott, R. L., E. A. Edwards, W. J. Shuttleworth, T. E. Huxman, C. Watts, and D. C. Goodrich, 2004: Interannual and seasonal variation in fluxes of water and carbon dioxide from a riparian woodland ecosystem. *Agric. For. Meteor.,* **122,** 65–84.

Stewart, J. B., C. J. Watts, and J. C. Rodriguez, 1998: Energy budget of range land vegetation in northwest Mexico. Preprints, *23d Conf. on Agricultural and Forest Meteorology,* Albuquerque, NM, Amer. Meteor. Soc., 258–261.

Twine, T. E., and Coauthors, 2000: Correcting eddy-covariance flux underestimates over a grassland. *Agric. For. Meteor.,* **103,** 279–300.